Propane Aromatization on Zn-Modified Zeolite BEA Studied by Solid-State NMR in Situ

ARTICLE *in* THE JOURNAL OF PHYSICAL CHEMISTRY C · JUNE 2010

Impact Factor: 4.77 · DOI: 10.1021/jp103580f

4 AUTHORS, INCLUDING:

Anton Gabrienko
Boreskov Institute of Catalysis
27 PUBLICATIONS **238** CITATIONS
SEE PROFILE

Dieter Freude
University of Leipzig
184 PUBLICATIONS **3,962** CITATIONS
SEE PROFILE

Alexander G Stepanov
Boreskov Institute of Catalysis
136 PUBLICATIONS **1,679** CITATIONS
SEE PROFILE

Propane Aromatization on Zn-Modified Zeolite BEA Studied by Solid-State NMR in Situ

Anton A. Gabrienko,[†] Sergei S. Arzumanov,[†] Dieter Freude,[‡] and Alexander G. Stepanov*,[†]

Boreskov Institute of Catalysis, Siberian Branch of the Russian Academy of Sciences, Prospekt Akademika Lavrentieva 5, Novosibirsk 630090, Russia, and Abteilung Grenzflächenphysik, Universität Leipzig, Linnéstrasse 5, 04103 Leipzig, Germany

Received: April 21, 2010; Revised Manuscript Received: June 17, 2010

The conversion of propane (propane-1-^{13}C and propane-2-^{13}C) on Zn/H-BEA zeolite at 520−620 K has been studied by ^{1}H and ^{13}C (CP) MAS NMR. Propene adsorption complex with zinc sites (π-complex) and σ-allylzinc species as intermediates have been identified in the course of propane conversion to aromatics. The mechanism leading to the formation of methane and ethane, which are constituents of an undesirable route in propane conversion, has been examined by kinetic modeling of the expected reaction network based on in situ ^{1}H MAS NMR kinetic measurements of the reaction performance. The pathways for propane aromatization and hydrogenolysis have been proposed. Hydrogenolysis of propane has been concluded to occur with the involvement of both Brønsted acid sites and Zn sites.

1. Introduction

Aromatization of propane and the other small alkanes represents a promising way to produce the highly valuable aromatic products from the saturated hydrocarbons.[1–5] The mechanism of propane aromatization over metal-modified (mainly Ga and Zn) zeolites has been widely addressed in the literature during the last decades with the aim of finding a pathway for the enhancement of aromatization efficiency.[1–7] The generally accepted reaction network includes propane dehydrogenation to form an olefin, which is further involved in dehydrooligomerization and cyclization steps to form aromatic molecules.[4] For the most frequently used catalysts based on high silica zeolites modified with gallium or zinc, the role of the metal component remains controversial. It may consist in a creation of the bifunctional sites performing propane activation[8] or an increase of the dehydrogenation function of the catalyst,[1,3,5,7] providing the easier way for hydrogen desorption as H_2.[4]

The formation of lower alkanes (methane, ethane) on Zn- and Ga-modified zeolites represents an undesirable route in the course of propane aromatization.[6] Most of the studies investigating the primary products of propane conversion claim a significance of a protolytic cracking mechanism for methane formation.[1,2,5] It was found that, upon decreasing the contact time, more ethane and methane were produced, and a hydrogenolysis of propane was proposed.[7,9] The occurrence of a direct hydrogenolysis of propane[10] and ethane[11] was claimed by analysis of the reaction products and the reaction kinetics with NMR in a batch reactor. However, the mechanism of this reaction on metal-modified zeolites is still poorly understood.

Solid-state NMR spectroscopy has demonstrated many times its efficiency in the characterization of hydrocarbon conversion on zeolite catalysts[8,10,12–25] and in situ monitoring the reaction kinetics.[11,26,27] In this paper, two methods of MAS NMR spectroscopy, ^{13}C CP/MAS NMR and ^{1}H MAS NMR in situ kinetic measurements, have been used to identify the steps of propane conversion on Zn-modified zeolite BEA leading to aromatic molecules and to clarify the mechanism, which offers the undesirable byproducts ethane and methane, influencing the alkane aromatization efficiency.

2. Experimental Section

2.1. Materials Characterization and Sample Preparation. The acid-form zeolite beta (H-BEA, Si/Al = 19) was synthesized by the procedure described in ref 28. The zinc form (Zn/H-BEA) was prepared by impregnation of the H-BEA sample with a saturated solution of zinc formate, subsequent drying at 473 K for 14 h, and further calcination at 673 K for 4 h in a flow of air. The Zn content in a final Zn/H-BEA zeolite was 5.6 wt %. Materials were characterized by XRD, SEM, TEM, UV−vis, and IR diffuse reflectance spectroscopy and ^{1}H, ^{27}Al, and ^{29}Si MAS NMR spectroscopies. The residual quantity of 420 μmol g^{-1} for the acidic AlOHSi groups in Zn/H-BEA was estimated by ^{1}H MAS NMR with adsorbed methane as an internal standard. The presence of a bulk ZnO phase in Zn/H-BEA was demonstrated by XRD analysis. Additionally, the UV−vis diffuse reflectance spectrum showed subnanometric ZnO clusters (the band at 265 nm) and macrocrystalline particles of ZnO on the extra surface of the zeolite (the band at 370 nm).[29] A more detailed characterization of zeolite Zn/H-BEA is provided in ref 30.

Propane-1-^{13}C, propane-2-^{13}C (both 99% ^{13}C enrichment), and propane C_3H_8 (purity ≥ 99%) were purchased from Aldrich Chemical Co. Inc. and used without further purification. The samples for NMR measurements were axially high symmetric sealed glass tubes with an outer diameter of 5.5 mm and length of 10 mm, containing 80 mg of the zeolite. The zeolite samples were activated under vacuum by an increase of the temperature from 300 to 673 K at the rate of 10 K h^{-1} and further maintained at 673 K for 24 h under vacuum (less than 10^{-2} Pa). Prior to sealing, the sample of zeolite was loaded with 320 μmol/g of propane at room temperature. This glass tube could be tightly inserted in a 7 mm zirconia MAS NMR rotor.

2.2. NMR Measurements. NMR spectra were recorded at 9.4 T on a Bruker Avance-400 spectrometer, equipped with a high-temperature broad-band double-resonance MAS probe. ^{13}C CP/MAS NMR spectra with cross-polarization (CP) and high-

* To whom correspondence should be addressed. Tel: +7 383 326 9437. Fax: +7 383 330 8056. E-mail: stepanov@catalysis.ru.
† Siberian Branch of the Russian Academy of Sciences.
‡ Universität Leipzig.

10.1021/jp103580f
Published on Web 06/30/2010

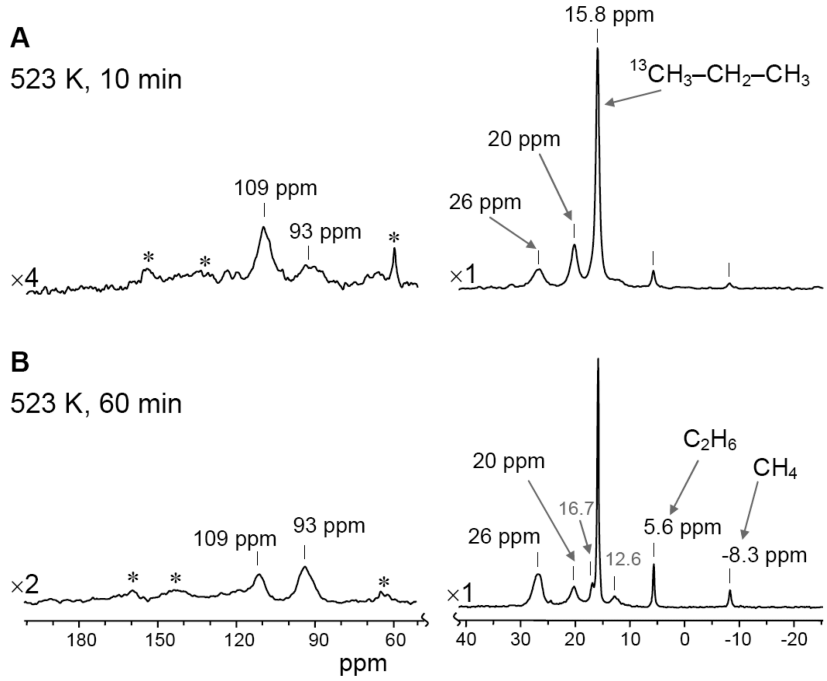

Figure 1. ^{13}C CP/MAS spectra of propane-1-^{13}C after reaction on Zn/H-BEA at 523 K. Asterisks (∗) denote spinning sidebands.

power proton decoupling were recorded at 100.613 MHz at 300 K. The proton high-power decoupling field strength was 11.7 G (5.0 μs length of 90° ^1H pulse); the contact time was 1−3 ms at the Hartmann−Hahn matching condition of 50 kHz. Scans (40 000) were accumulated for a spectrum with the delay time between scans of 3 s. ^1H MAS NMR spectra were recorded at 400.13 MHz by a Hahn-echo pulse sequence of $\pi/2-\tau-\pi-\tau$, where τ equals one rotor period. The excitation pulse length was 4.5 μs ($\pi/2$), and 24 scans were accumulated for a spectrum with a 4−6 s delay. The T_1 for methane and ethane were 400 and 310 ms at 555 K. This made possible a quantitative estimate of signal intensities in the ^1H MAS NMR spectra. Zirconia rotors (7 mm) with inserted sealed glass tubes were spun at 3−5 kHz by dried compressed air at 300−555 K.

In situ kinetic measurements were performed with ^1H MAS NMR at 524−555 K. Before acquisition of the signal, the NMR probe with the sample was preheated for 20 min at the temperature at which the conversion of propane did not yet occur at a notable rate. The temperature was then increased within 8 min by 50−100 K to the reaction temperature, equilibrated for 2−5 min, and then the acquisition of the NMR signal started. The time interval for successive spectra during kinetic measurements was 5−10 min depending on the reaction rate.

The chemical shifts were referenced to an external TMS standard. The sample temperature was controlled by the Bruker BVT-2000 variable-temperature unit. The calibration of the temperature inside the rotor was performed with an accuracy of ±2 K by the use of lead nitrate as a ^{207}Pb MAS NMR chemical shift thermometer.[31]

2.3. Kinetic Analysis. The kinetics obtained with ^1H MAS NMR were analyzed within the frame of a proposed reaction network (Schemes 2 and 3). Simulated kinetic curves were calculated by the semiimplicit Runge−Kutta method for integration of sets of stiff equations with an integration step adaptation.[32] Rate constants were determined by fitting of the simulated kinetic curves to the experimentally obtained curves using the rate constants as free parameters.

3. Results and Discussion

3.1. Conversion of Propane Studied by ^{13}C MAS NMR. Figure 1 shows ^{13}C CP/MAS NMR spectra of propane-1-^{13}C after reaction at 523 K on Zn/H-BEA zeolite. The intense resonance at 15.8 ppm arises from the ^{13}C-labeled methyl groups of the initial propane. Four weaker signals appear at 109, 93, 26, and 20 ppm after 10 min of reaction time at 523 K (Figure 1A). The signals at 93 and 26 ppm increase in intensity at longer reaction times (Figure 1B).

A similar experiment was done with propane-2-^{13}C adsorbed on Zn/H-BEA. Because of the location of the selective ^{13}C label in the CH_2 group, the signal from the initial propane is observed at 16.7 ppm (Figure 2). A relatively weak and broad signal appears at 165 ppm after 10 min of heating at 523 K (Figure 2A). Further transformation causes the resonances at 93 and 26 ppm (Figure 2B).

At the reaction temperature of 553−623 K, ^{13}C MAS NMR spectra are almost similar for both propane-1-^{13}C and propane-2-^{13}C (Figure 3). This should be the result of an essentially uniform distribution of the ^{13}C label among the reaction products at these temperatures due to its scrambling. At the reaction temperature of 623 K, mainly the signals from the simple methyl-substituted aromatics (toluene, xylenes) at 131 and 19 ppm, ethane (5.6 ppm), and methane (−8.2 and −11.2 ppm) are observed in the spectra, a noticeable amount of more condensed aromatics (ca. 150 ppm) being also present (Figure 3B).

The spectra in Figures 1 and 2 reveal several signals that disappear at $T > 523$ K. These signals should be related to the intermediate species formed in the course of propane conversion to aromatics. Different signals, observed for the intermediates formed from propane-1-^{13}C and propane-2-^{13}C, arise from different ^{13}C-labeled fragments of these intermediates. According to the order of their appearance, the signals at 109 and 20 ppm formed from propane-1-^{13}C (Figure 1) and the signal at 165 ppm formed from propane-2-^{13}C (Figure 2) are assigned to the first intermediate. The signals at 93 and 26 ppm belong to the

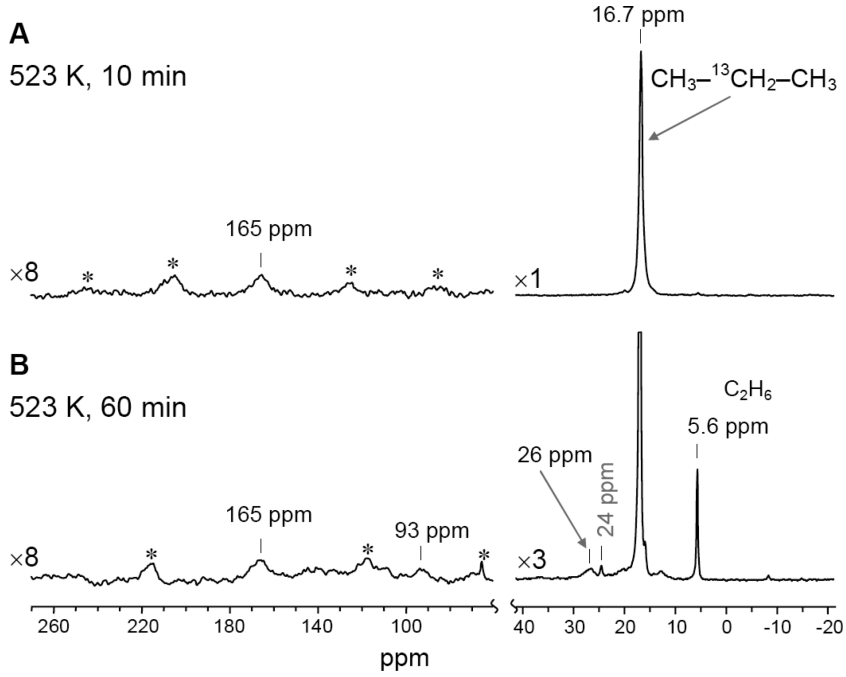

Figure 2. ^{13}C CP/MAS spectra of propane-2-^{13}C after reaction on Zn/H-BEA at 523 K. Asterisks (∗) denote spinning sidebands.

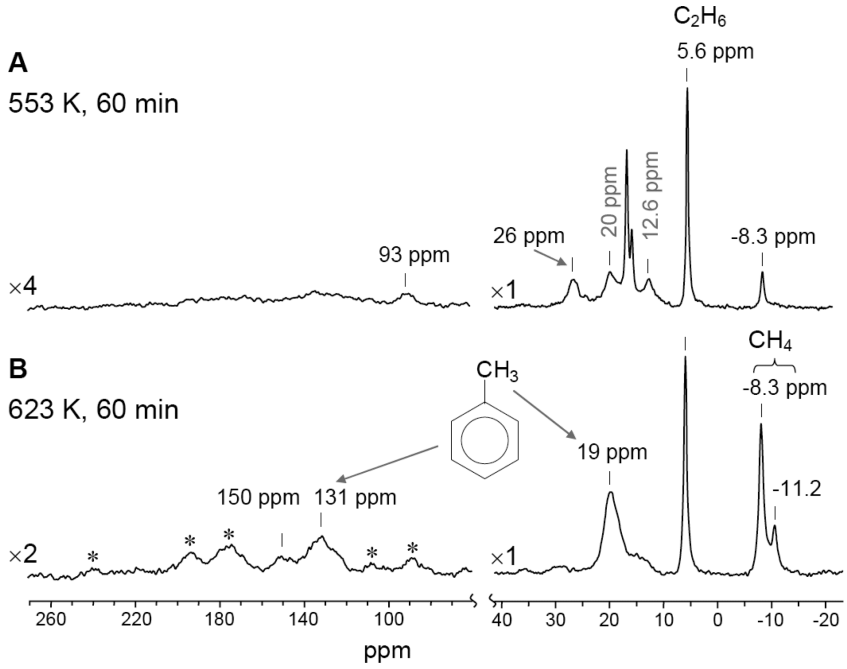

Figure 3. ^{13}C CP/MAS spectra of propane-2-^{13}C on Zn/H-BEA after reaction at 553 and 623 K. Asterisks (∗) denote spinning sidebands.

second intermediate that is formed concurrently with the degradation of the first one. It is seen from Figure 1 that these two signals increase at the expense of the loss of the intensity of the resonances at 109 and 20 ppm, thus evidencing the transformation of the first intermediate into the second one.

The signals 109 (CH_2═), 165 (═CH−), and 20 ppm (CH_3−) can be assigned to the adsorptive complex of propene with zinc sites; the corresponding resonances from the gaseous propene were reported to be at 114.7, 135.0, and 19.0 ppm.[33] The essential downfield shift of the signal from the ═CH− group as compared with gaseous propene by 30 ppm may arise from the strong interaction of a propene double bond with Zn sites. The shift of the signals at a double bond does not exceed 10 ppm at the weak interaction of an olefin double bond with Brønsted acid sites[22,34] or Na^+ cations.[35] Similar signals for the products of propane conversion on zinc-loaded zeolite MFI were identified by Ivanova et al.[36] They assigned these signals to the asymmetric π complex of propene with zinc cations.

We assign the signals at 93 and 26 ppm to zincallyl fragments. Such species are known to arise from the interaction of propene with zinc oxide. IR[37,38] and NMR[39] studies showed an η^3 structure (π-allyl) for the zincallyl fragment formed on bulk zinc oxide. However, according to Benn et al.,[40] the η^1 structure (i.e., σ-allyl) becomes more favorable for zincallyl species in the presence of donor molecules. It can be proposed that the signals at 93 and 26 ppm in Figure 1 belong to C_3 and C_1 carbons of zincallyl species, which is of an η^1 structure due to the donor effect of oxygen of the zeolite framework on the electron structure of zinc species inside zeolite pores. It seems that C_2 carbons in both the propene coordinated to the Zn sites

and the σ-allylzinc species exhibit broad signals with similar chemical shifts at 165 ppm. This is a reasonable suggestion because the signal at 165 ppm displays no change in intensity upon transformation of propene into an σ-allyl fragment when two couples of the signals 109, 20 ppm and 93, 26 ppm change their intensities upon this transformation. Three signals at 93, 165, and 26 ppm thus assigned to σ-allylzinc species are indeed in a close vicinity to the range of chemical shifts reported for some zincallyl species having an η^1 structure, which are 98−100 ppm for C_1 carbons, 145−153 ppm for C_2 carbons, and 20−24 ppm for C_3 carbons.[40]

The signals at 92 and 26 ppm were earlier detected for propane conversion on Zn-MFI.[36] The resonance at 26 ppm was assigned to the methylene group of *n*-butane. This assignment is doubtful as the signals from other alkanes in the same spectrum were narrower (see Figure 2 in ref 36). Also, the signal at 26 ppm was enhanced significantly by cross-polarization, which is accounted for by rigidly bound species rather than weakly bonded to the zeolite framework alkane. As further evidence against *n*-butane, Figure 1 of this study shows that the signal at 26 ppm and the signal at 12.5 ppm, which could be attributed to the methyl groups of *n*-butane, are not equal in their intensities. Furthermore, in the presence of a zeolite catalyst, containing Brønsted acid sites, *n*-butane, if forms, converts rapidly to isobutane.[41] In line with this, we have observed a very small and narrow signal at 24 ppm, pointing to a possible formation of isobutane (Figure 2B). The 24 ppm signal, however, is registered at a very limited temperature range of propane conversions, apparently due to further transformations of isobutane. Thus, a broad signal at 26 ppm observed in ^{13}C CP/MAS spectra cannot arise from *n*-butane.

The signal at 92 ppm was attributed by Ivanova et al.[36] to odd-numbered carbons in delocalized carbanions, whereas the even-numbered carbons displayed the signal at 140 ppm in their study. That assignment was substantiated by the fact that both signals appeared at the same time. In the present study for propane conversion on Zn/H-BEA zeolite, we never observed the signal at 140 ppm. In this study, we do not confirm the formation of delocalized carbanionic species as intermediates of propane aromatization on Zn-modified zeolite BEA.

Figures 1 and 2 reveal the beginning of the ^{13}C-label scrambling process for propane on Zn/H-BEA at 523 K. The appearance of the signals at 16.7 ppm in Figure 1B and at 15.8 ppm in Figure 2B evidences the exchange of the ^{13}C label between the methyl and the methylene groups of propane. The scrambling of the ^{13}C label indicates involvement of Brønsted acid sites,[26] though propane conversion into propene due to interaction with zinc sites occurs to a larger extent under these conditions. The scrambling of ^{13}C labels is also identified for σ-allylzinc species. In Figure 2B, the weak signals at 26 and 93 ppm from the ^{13}C labels in the C_1 and C_3 positions of σ-allylzinc are identified due to a transfer of the ^{13}C label from the C_2 position with the signal at 165 ppm. We were not able to find a distinct resonance at 165 ppm in Figure 1, which would confirm the reverse process of the ^{13}C-label scrambling from the C_1 (or C_3) into the C_2 position of σ-allylzinc. The probable reason is a large width of this signal resulting in more sidebands, which could make the signal undetectable.

The formation of intermediate *n*-propylzinc species exhibiting the signals 12.2, 19.5, and 20.3 ppm was reported as the first step of propane conversion on Zn/MFI catalyst.[10,36] An *n*-propylzinc species on Zn/MFI was also identified earlier by IR spectroscopy.[42,43] Interestingly, in this study, such a species was not found at the beginning of propane conversion on Zn/H-BEA at 523 K. Nevertheless, at $T > 523$ K, we have observed the gradually increasing signals at 12.6 and 20.0 ppm that could be assigned to *n*-propylzinc fragments. Such an observation may indicate a higher reactivity of *n*-propylzinc species in zeolite Zn/H-BEA toward further conversions to propene and σ-allylzinc species. An accumulation of *n*-propylzinc species becomes possible because zeolite Brønsted sites, which are involved in the further *n*-propylzinc transformation to propene[44] and possibly σ-allylzinc species, could be deactivated by the formed allene oligomers and aromatics.

At 553 K, the signals from the intermediate propene and σ-allylzinc species vanish and the olefinic part of the ^{13}C NMR spectrum (Figure 3A) becomes featureless, possibly due to formation of oligomeric species from propene and σ-allylzinc, and oligomeric species evolve further to aromatics.

The observed intermediates and products imply that propane transformation to aromatics occurs in accordance to pathway 1 of Scheme 1.

At the first step, a dissociative adsorption of propane on ZnO species located in the channels of the zeolite occurs to form *n*-propylzinc species. Further hydrogen abstraction with the involvement of Brønsted acid sites occurs to give propene. The formed propene does not leave the Zn site but remains in a strong interaction with this site by π bonding. Otherwise, propene must be oligomerized on a neighbor acid site.[12] The π complex of propene transforms further to σ-allylzinc species. Dehydrogenation of the latter with possible participation of a neighbor Brønsted site (similar to hydrogen abstraction from *n*-propylzinc species) produces probably allene. Oligomerization of allene on Brønsted acid sites and further dehydrogenation and cyclization give rise the aromatic molecules. Note that the characteristic ^{13}C NMR signals from allene[33] at 210 and 75 ppm were not detected in the spectra, which is accounted for by its fast oligomerization and further conversion to aromatics.

3.2. Analysis of the Kinetics of Propane Conversion with ^1H MAS NMR. A significant amount of ethane and methane is produced from propane, starting from the very beginning of propane conversion (Figures 1−3). Concurrent to the aromatization process, a formation of ethane and methane was assumed to result from the direct hydrogenolysis of propane on zinc sites.[10] Methane and ethane can be alternatively formed via dealkylation or side-chain hydrogenolysis of initially formed bulky aromatic molecules; such a process may involve acidic and/or metal sites of zeolites modified with transition metals.[45]

We further performed an analysis of the kinetics of propane conversion with the aim of verifying the possibility of the formation of a notable amount of methane and ethane by propane hydrogenolysis. The analysis has been carried out based on ^1H MAS NMR data obtained in situ under the conditions of a batch reactor. Figure 4 shows that a time dependence is observed for several signals: two resonances from propane at 1.0 and 1.5 ppm decrease while the signals from methane at ca. 0.1 ppm increase. The variation of signal intensity at ca. 1.0 ppm has a contribution from both a decreasing signal of the propane methyl groups and an increasing signal of ethane. A deconvolution of the signal at 1.0 ppm for two components allows deriving the kinetic curves for both propane and ethane (Figure 5A). Because of their large width and small intensity, no signals from aromatics and other intermediate products (oligomers) formed also in the reaction are detected in ^1H MAS NMR spectra during kinetic measurements. However, the kinetic curves for hydrogen and carbon atoms in aromatics and other invisible by NMR products can be derived (Figure 5B) from the confrontation of the experimental ^1H MAS NMR intensities

SCHEME 1: Proposed Pathways for Propane Aromatization and Hydrogenolysis on Zeolite Zn/H-BEA

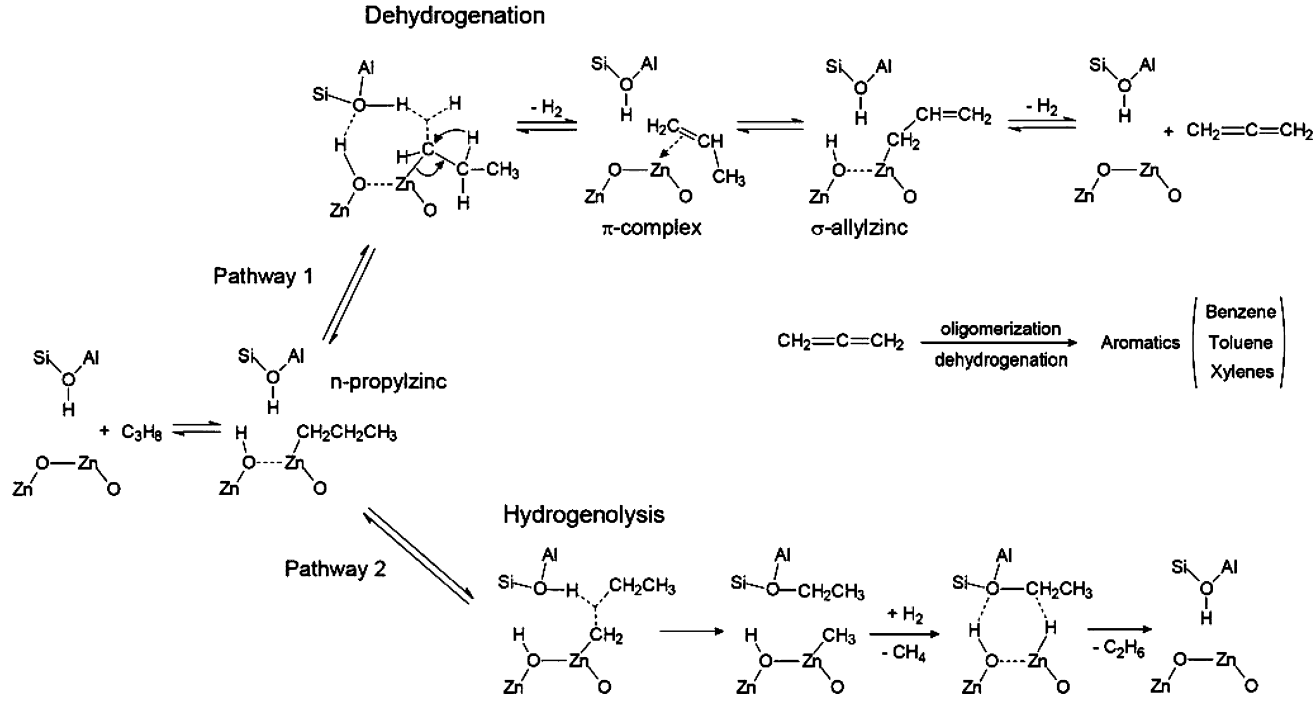

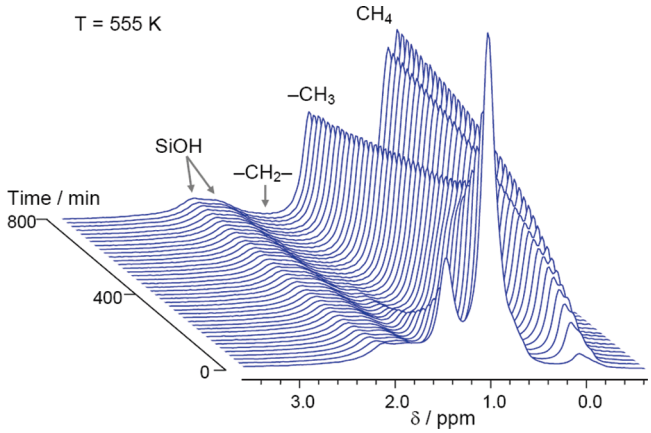

Figure 4. Stack plot of ^{1}H MAS NMR spectra of propane on zeolite Zn/H-BEA. $T = 555$ K.

for propane, ethane, and methane with the initial quantity of propane introduced in the sample.

An approximately equal quantity of methane and ethane is evolved at the beginning of the reaction. At the reaction time longer than 100 min, methane becomes a prevailing product (Figure 5); the quantity of the evolved ethane slowly decreases. The decrease of ethane evolution is due to the occurrence of the reaction of ethane conversion to aromatics and its hydrogenolysis to methane, as clearly demonstrated earlier.[11] We have further analyzed the kinetics of propane conversion and methane and ethane formation (Figures 5 and 6) in the frame of two alternative kinetic schemes (Schemes 2 and 3). Scheme 2 includes the expected basic stages, described by the rate constants k_1, k_{-1}, k_2, and k_5, for propane conversion to aromatics and its conversion to methane and ethane by the hydrogenolysis reaction. The rate constants k_3, k_{-3}, k_4, and k_6 that describe the stages of ethane dehydrogenation, hydrogenolysis, and aromatization were adapted from the earlier study of ethane conversion on Zn/H-BEA.[11]

Thus, there are four free kinetic parameters (k_1, k_{-1}, k_2, k_5) in Scheme 2 to perform a fitting to the experimental kinetic curves. To keep the number of free fitting parameters as low as possible, the intermediate steps involving oligomeric species preceding aromatics and other surface species (such as olefins adsorbed on zinc sites or zincallyl fragments) were omitted in Scheme 2. The formation of other aromatic products apart from toluene (C_7H_8) is ignored as well. Simulated kinetic curves for propane, ethane, and methane are shown in Figure 5. A close coincidence achieved for simulated and experimental curves makes it reasonable to rationalize a propane conversion as proceeding in accordance to Scheme 2, including two main routes: propane dehydrogenation and propane hydrogenolysis. The latter process consumes hydrogen formed in the former process. Estimation of the activation energies on the basis of Scheme 2 offers a value of 72 ± 18 kJ mol^{-1} for propane dehydrogenation and 80 ± 15 kJ mol^{-1} for propane hydrogenolysis. These estimates are close to the values earlier reported for propane dehydrogenation on pure acid-form H-ZSM-5 zeolite (apparent activation energy was found to be 70−95 kJ mol^{-1}[46,47]) and for the overall propane conversion on Ga-modified ZSM-5 (ca. 81 kJ mol^{-1}[48]).

Hydrogenolysis of side chains in bulk aromatic molecules represents an alternative route to methane (ethane) formation.[45] To explore this possibility, we have performed the modeling of the kinetics in accordance to Scheme 3. The scheme includes a conversion of propane to bulk aromatic products (alkyl-substituted benzenes $C_{(7+a)}H_{(8+2a)}$), followed by successive dealkylation to yield finally methane, ethane, and toluene. Additionally, Scheme 3 includes the stage of ethane hydrogenolysis[11] (k_5) to explain the diminishing of the ethane curve in the final part of the kinetics. The results of kinetic modeling have shown that parameter a should be ≥10, which means that at least 10 carbons are to be split off from alkyl substituents in the intermediate aromatic product. A shorter length for alkyl side chains in this product (i.e., $a < 10$) makes a high yield of methane and ethane impossible to fit the experimentally observed kinetics.

Figure 6 shows the kinetic modeling performed on the basis of Scheme 3, assuming that a bulky aromatic product of the

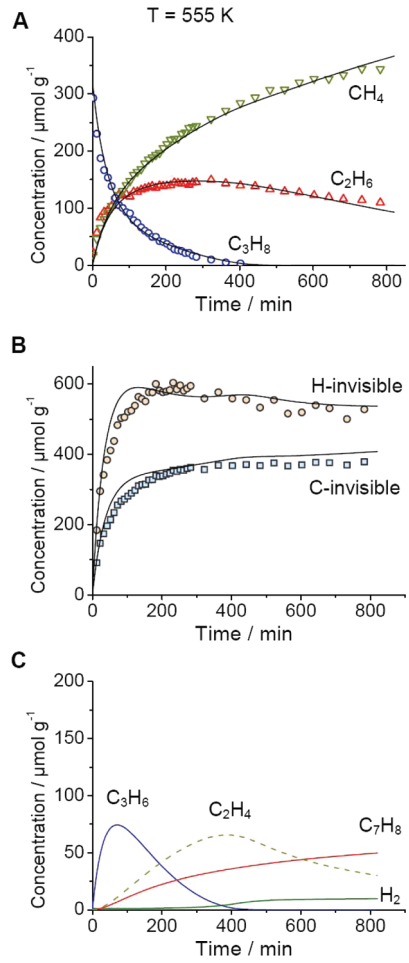

Figure 5. Modeling of the experimental kinetics of propane conversion on zeolite Zn/H-BEA, performed on the basis of Scheme 2 ($T = 555$ K). Experimental and simulated kinetics for (A) propane, ethane, and methane and (B) invisible by NMR hydrogen and carbon atoms in the intermediate species (propene, ethene) and the products (aromatics and H_2). Solid curves represent the simulated kinetics with parameters $k_1 = 0.01$ min^{-1}, $k_{-1} = 0.01$ g μmol^{-1} min^{-1}, $k_2 = 0.008$ g μmol^{-1} min^{-1}, $k_3 = 0.0025$ min^{-1}, $k_{-3} = 0.0007$ g μmol^{-1} min^{-1}, $k_4 = 0.0001$ g μmol^{-1} min^{-1}, $k_5 = 0.004$ min^{-1}, and $k_6 = 0.0025$ min^{-1}. (C) Simulated kinetics for products (propene, ethene, H_2, and toluene), invisible by NMR; the sum of these curves corresponds to the kinetic curves in (B).

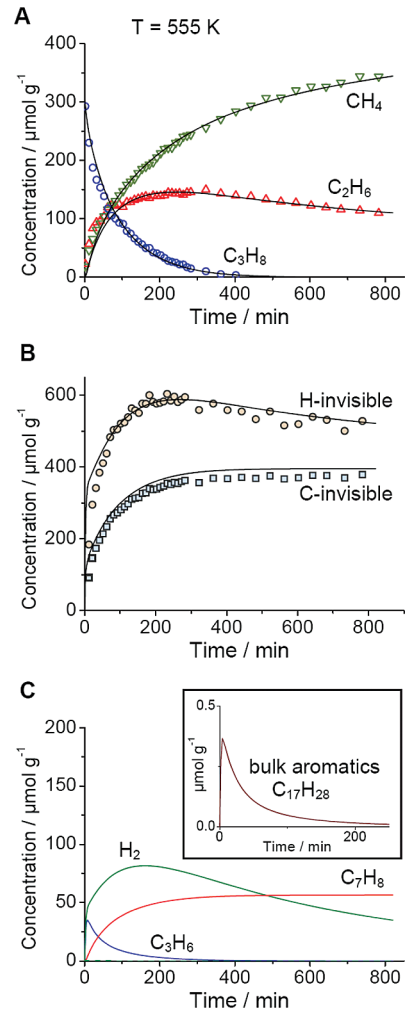

Figure 6. Modeling of the experimental kinetics of propane conversion on zeolite Zn/H-BEA, performed on the basis of Scheme 3 ($T = 555$ K). The corresponding rate constants are $k_1 = 0.04$ min^{-1}, $k_{-1} = 0.004$ g μmol^{-1} min^{-1}, $k_2 = 0.12$ min^{-1}, $k_3 = 0.017$ g μmol^{-1} min^{-1}, $k_4 = 0.032$ min^{-1}, and $k_5 = 0.000012$ g μmol^{-1} min^{-1}; parameter a is equal to 10.

composition $C_{17}H_{28}$ (e.g., tri-isopropyl-ethyl-benzene) is formed. An extremely fast formation (k_2) and conversion (k_3, k_4) should be proposed for this intermediate aromatic product in order to exclude an induction period in the methane and ethane kinetic curves. Under such conditions, Scheme 3 predicts a significant production of dihydrogen (ca. 40−70 μmol g^{-1}, Figure 6B), which is a contradiction to the experimental results. Indeed, ^{1}H MAS NMR spectra in Figure 4 show a complete absence of the signal from molecular H_2 (4.1 ppm[49]). This fact makes Scheme 3 less reasonable despite a good correspondence achieved between the experimental and the simulated kinetics for propane, ethane, and methane (Figure 6A). Thus, we conclude that methane and ethane production on zeolite Zn/H-BEA cannot occur exclusively by the route of side-chain hydrogenolysis in bulky aromatic molecules. This result favors a hypothesis considered in Scheme 2; that is, methane and ethane are formed by hydrogenolysis of a propane molecule.

The process of alkane hydrogenolysis is classically thought to occur through formation of a surface species with multiple metal−carbon bonds, which allows a rupture of a weaken carbon−carbon bond.[50,51] For such a process to occur, the metal

SCHEME 2: Kinetic Scheme for Propane Conversion by Aromatization and Hydrogenolysis

$$C_3H_8 \underset{k_{-1}}{\overset{k_1}{\rightleftharpoons}} C_3H_6 + H_2$$

$$C_3H_8 + H_2 \xrightarrow{k_2} C_2H_6 + CH_4$$

$$C_2H_6 \underset{k_{-3}}{\overset{k_3}{\rightleftharpoons}} C_2H_4 + H_2$$

$$C_2H_6 + H_2 \xrightarrow{k_4} 2\,CH_4$$

$$C_3H_6 \xrightarrow{k_5} 3/7\,C_7H_8 + 9/7\,H_2$$

$$C_2H_4 \xrightarrow{k_6} 2/7\,C_7H_8 + 6/7\,H_2$$

surface is needed. One could suppose that zinc oxide, which is present in the Zn/H-BEA sample, is reduced to metallic zinc by H_2 formed at propane dehydrogenation. However, the reduction of ZnO to metallic Zn by H_2 does not occur under conditions of our experiment due to the thermodynamic limitations.[52] Therefore, the hypothesis of propane hydrogenolysis on the surface of zinc metal does not satisfy our experimental data. It has been discussed in the literature that methane formation

SCHEME 3: Kinetic Scheme for Methane and Ethane Formation via Hydrogenolysis of Side Chains in Bulk Aromatics

$$C_3H_8 \underset{k_{-1}}{\overset{k_1}{\rightleftharpoons}} C_3H_6 + H_2$$

$$C_3H_6 \xrightarrow{k_2} \frac{3}{(7+a)} C_{(7+a)}H_{(8+2a)} + \frac{9}{(7+a)} H_2$$

$$C_{(7+a)}H_{(8+2a)} + a\ H_2 \xrightarrow{k_3} C_7H_8 + a\ CH_4$$

$$C_{(7+a)}H_{(8+2a)} + \left(\frac{a}{2}\right) H_2 \xrightarrow{k_4} C_7H_8 + \left(\frac{a}{2}\right) C_2H_6$$

$$C_2H_6 + H_2 \xrightarrow{k_5} 2\ CH_4$$

under aromatization conditions may occur via protolytic cracking of propane on Brønsted acid sites of metal-modified zeolite.[2] However, the metal sites of metal-modified zeolites can be involved in methane generation, as followed from the mechanism suggested by Ono[5] for Zn/ZSM-5 and kinetics modeling performed by Lukyanov et al.[45] for propane conversion on Ga/H-ZSM-5. Although methane is produced directly from propane, ethane production may include a hydrogenation of ethene, formed in one step with methane, by H_2 on metal sites.[45]

Our recent studies of H/D exchange between C_1-C_4 alkanes and zeolite Brønsted acid sites on Zn-modified high silica zeolites (ZSM-5 and BEA) have shown a strong influence of Zn on the activation of C−H bonds by zeolite Brønsted sites: a reversible process of the cleavage and the formation of alkane C−H bonds occurs easily if zeolite is modified with Zn.[44,53,54] It has been concluded that both Zn sites and Brønsted sites can be involved in a first step of alkane aromatization−alkane dehydrogenation to form olefin,[43] as shown in Scheme 1, pathway 1. It is reasonable to assume that the formation of a notable amount of both methane and ethane on Zn/H-BEA also occurs with the involvement of both Zn sites and Brønsted sites, as shown in Scheme 1, pathway 2. A cleavage of the C−C bond in *n*-propylzinc species formed at the dissociative adsorption of propane seems to occur easily due to the protonation of the C−C bond by a Brønsted acid site located in the vicinity of a Zn site at which a dissociative adsorption of the alkane is performed. This gives rise to methane and ethane as byproducts of propane aromatization.

4. Conclusions

In situ NMR analysis of the intermediates, the products, and the reaction kinetics allows us to make the following conclusion on propane conversion on Zn-modified zeolite BEA. The transformation of propane occurs by two competitive pathways, aromatization and hydrogenolysis. Propene adsorption complex with zinc sites (π-complex) and σ-allylzinc species are successive intermediates toward aromatics, evolved probably from *n*-propylzinc species[10] formed at the dissociative adsorption of propane on ZnO species inside the pores of the zeolite. Ethane formed under propane hydrogenolysis is further involved in aromatization and hydrogenolysis as well.[11] Involvement of both Brønsted acid sites and Zn sites in alkane activation, which facilitates a cleavage of C−C bonds,[44] gives rise to a notable formation of methane and ethane by a hydrogenolysis process.

Acknowledgment. This work was supported by the Russian Foundation for Basic Research (Grant No. 10-03-00555). S.S.A. is grateful to the Russian Science Support Foundation for financial support. A.A.G. thanks the Zamaraev International Charitable Foundation for financial support.

References and Notes

(1) Bhan, A.; Delgass, W. N. *Catal. Rev.−Sci. Eng.* **2008**, *50*, 19–151.
(2) Caeiro, G.; Carvalho, R. H.; Wang, X.; Lemos, M. A. N. D. A.; Lemos, F.; Guisnet, M.; Ramoa Ribeiro, F. *J. Mol. Catal. A: Chem.* **2006**, *255*, 131–158.
(3) Hagen, A.; Roessner, F. *Catal. Rev.−Sci. Eng.* **2000**, *42*, 403–437.
(4) Biscardi, J. A.; Iglesia, E. *Catal. Today* **1996**, *31*, 207–231.
(5) Ono, Y. *Catal. Rev.−Sci. Eng.* **1992**, *34*, 179–226.
(6) Biscardi, J. A.; Iglesia, E. *J. Catal.* **1999**, *182*, 117–128.
(7) Seddon, D. *Catal. Today* **1990**, *6*, 351–372.
(8) Derouane, E. G.; Hamid, S. B. A.; Ivanova, I. I.; Blom, N.; Hojlundnielsen, P. E. *J. Mol. Catal.* **1994**, *86*, 371–400.
(9) Mole, T.; Anderson, J. R.; Creer, G. *Appl. Catal.* **1985**, *17*, 127–141.
(10) Kolyagin, Y. G.; Ordomsky, V. V.; Khimyak, Y. Z.; Rebrov, A. I.; Fajula, F.; Ivanova, I. I. *J. Catal.* **2006**, *238*, 122–133.
(11) Arzumanov, S. S.; Gabrienko, A. A.; Freude, D.; Stepanov, A. G. *Solid State Nucl. Magn. Reson.* **2009**, *35*, 113–119.
(12) Haw, J. F.; Richardson, B. R.; Oshio, I. S.; Lazo, N. D.; Speed, J. A. *J. Am. Chem. Soc.* **1989**, *111*, 2052–2058.
(13) Anderson, M. W.; Klinowski, J. *Nature* **1989**, *339*, 200–203.
(14) Stepanov, A. G.; Zamaraev, K. I.; Thomas, J. M. *Catal. Lett.* **1992**, *13*, 407–422.
(15) Stepanov, A. G. *Catal. Today* **1995**, *24*, 341–348.
(16) Stepanov, A. G.; Sidelnikov, V. N.; Zamaraev, K. I. *Chem.−Eur. J.* **1996**, *2*, 157–167.
(17) Stepanov, A. G.; Luzgin, M. V. *Chem.−Eur. J.* **1997**, *3*, 47–56.
(18) Haw, J. F. *Top. Catal.* **1999**, *8*, 81–86.
(19) Derouane, E. G.; He, H. Y.; Derouane-Abd Hamid, S. B.; Ivanova, I. I. *Catal. Lett.* **1999**, *58*, 1–19.
(20) Hunger, M.; Weitkamp, J. *Angew. Chem., Int. Ed.* **2001**, *40*, 2954–2971.
(21) Luzgin, M. V.; Stepanov, A. G.; Shmachkova, V. P.; Kotsarenko, N. S. *J. Catal.* **2001**, *203*, 273–280.
(22) Stepanov, A. G.; Luzgin, M. V.; Arzumanov, S. S.; Ernst, H.; Freude, D. *J. Catal.* **2002**, *211*, 165–172.
(23) Luzgin, M. V.; Arzumanov, S. S.; Shmachkova, V. P.; Kotsarenko, N. S.; Rogov, V. A.; Stepanov, A. G. *J. Catal.* **2003**, *220*, 233–239.
(24) Luzgin, M. V.; Rogov, V. A.; Arzumanov, S. S.; Toktarev, A. V.; Stepanov, A. G.; Parmon, V. N. *Angew. Chem., Int. Ed.* **2008**, *47*, 4559–4562.
(25) Wang, W.; Hunger, M. *Acc. Chem. Res.* **2008**, *41*, 895–904.
(26) Arzumanov, S. S.; Reshetnikov, S. I.; Stepanov, A. G.; Parmon, V. N.; Freude, D. *J. Phys. Chem. B* **2005**, *109*, 19748–19757.
(27) Stepanov, A. G.; Arzumanov, S. S.; Ernst, H.; Freude, D. *Chem. Phys. Lett.* **2006**, *420*, 574–576.
(28) Schmidt, W.; Toktarev, A.; Schueth, F.; Ione, K. G.; Unger, K. *Stud. Surf. Sci. Catal.* **2001**, *135*, 311–318.
(29) Chen, J.; Feng, Z.; Ying, P.; Li, C. *J. Phys. Chem. B* **2004**, *108*, 12669–12676.
(30) Gabrienko, A. A.; Danilova, I. G.; Arzumanov, S. S.; Toktarev, A. V.; Freude, D.; Stepanov, A. G. *Microporous Mesoporous Mater.* **2010**, *131*, 210–216.
(31) Ferguson, D. B.; Haw, J. F. *Anal. Chem.* **1995**, *67*, 3342–3348.
(32) Villadsen, J.; Michelsen, M. L. *Solution of Differential Equation Models by Polynomial Approximation*; Prentice-Hall, Inc.: Englewood Cliffs, NJ, 1978.
(33) Breitmaier, E.; Voelter, W. *^{13}C NMR Spectroscopy, Methods and Applications in Organic Chemistry*; VCH: Weinheim, Germany, 1978.
(34) Stepanov, A. G.; Arzumanov, S. S.; Luzgin, M. V.; Ernst, H.; Freude, D. *J. Catal.* **2005**, *229*, 243–251.
(35) Michel, D.; Meiler, W.; Pfeifer, H. *J. Mol. Catal.* **1975**, *1*, 85–91.
(36) Ivanova, I. I.; Kolyagin, Y. G.; Ordomsky, V. V.; Asachenko, E. V.; Pasynkova, E. M.; Pirogov, Y. A. *J. Mol. Catal. A: Chem.* **2009**, *305*, 47–53.
(37) Dent, A. L.; Kokes, R. J. *J. Am. Chem. Soc.* **1970**, *92*, 1092–1093.
(38) Dent, A. L.; Kokes, R. J. *J. Am. Chem. Soc.* **1970**, *92*, 6709–6718.
(39) Kheir, A. A.; Howard, T.; Haw, J. F. *J. Am. Chem. Soc.* **1994**, *116*, 10839–10840.
(40) Benn, R.; Grondey, H.; Lehmkuhl, H.; Nehl, H.; Angermund, K.; Kruger, C. *Angew. Chem., Int. Ed.* **1987**, *26*, 1279–1280.
(41) Luzgin, M. V.; Stepanov, A. G.; Arzumanov, S. S.; Rogov, V. A.; Parmon, V. N.; Wang, W.; Hunger, M.; Freude, D. *Chem.−Eur. J.* **2006**, *12*, 457–465.
(42) Kazansky, V. B.; Serykh, A. I.; Pidko, E. A. *J. Catal.* **2004**, *225*, 369–373.
(43) Kazansky, V. B.; Pidko, E. A. *J. Phys. Chem. B* **2005**, *109*, 2103–2108.
(44) Stepanov, A. G.; Arzumanov, S. S.; Gabrienko, A. A.; Parmon, V. N.; Ivanova, I. I.; Freude, D. *ChemPhysChem* **2008**, *9*, 2559–2563.

(45) Lukyanov, D. B.; Gnep, N. S.; Guisnet, M. *Ind. Eng. Chem. Res.* **1995**, *34*, 516–523.
(46) Narbeshuber, T. F.; Vinek, H.; Lercher, J. A. *J. Catal.* **1995**, *157*, 388–395.
(47) Wang, X.; Carabineiro, H.; Lemos, F.; Lemos, M. A. N. D. A.; Ribeiro, F. R. *J. Mol. Catal. A: Chem.* **2004**, *216*, 131–137.
(48) Harris, J. L.; Krisko, N.; Wang, X. M. *Appl. Catal., A* **1992**, *83*, 59–74.
(49) Luzgin, M. V.; Stepanov, A. G.; Sassi, A.; Sommer, J. *Chem.—Eur. J.* **2000**, *6*, 2368–2376.
(50) Davis, B. H. *Catal. Today* **1999**, *53*, 443–516.
(51) Cortright, R. D.; Watwe, R. M.; Spiewak, B. E.; Dumesic, J. A. *Catal. Today* **1999**, *53*, 395–406.
(52) Taylor, G. B.; Starkweather, H. W. *J. Am. Chem. Soc.* **1930**, *52*, 2314–2325.
(53) Stepanov, A. G.; Arzumanov, S. S.; Parmon, V. N.; Kolyagin, Y. G.; Ivanova, I. I.; Freude, D. *Catal. Lett.* **2007**, *114*, 85–90.
(54) Stepanov, A. G.; Arzumanov, S. S.; Gabrienko, A. A.; Toktarev, A. V.; Parmon, V. N.; Freude, D. *J. Catal.* **2008**, *253*, 11–21.

JP103580F